Overview of JET Results

JET EFDA Contributors (see Annex 1.)

Presented by J. Paméla

EFDA Close Support Unit, Culham Science Centre, Abingdon, Oxon, OX14 3EA, UK

e-mail contact of main author: Jerome.Pamela@jet.efda.org

Abstract: scientific and technical activities on JET focus on the issues likely to affect the ITER design and operation. The physics of the ITER reference mode of operation, the ELMy H-mode, has progressed significantly: the extrapolation of ELM size to ITER has been re-evaluated; NTMs have been shown to be meta-stable in JET, and can be avoided via sawtooth destabilisation by ICRH; α-simulation experiments were carried out by accelerating ^{4}He beam ions by ICRH, providing a new tool for fast particle and MHD studies with up to 80-90% of plasma heating by fast ^{4}He ions. With or without impurity seeding, quasi-steady sate high confinement (H_{98}=1), high density (n_e/n_{GR} = 0.9-1) and high β (β_N=2) ELMy H-mode has been achieved by operating near the ITER triangularity (δ~0.40-0.5) and safety factor (q_{95}~3), at Z_{eff}~1.5-2. In Advanced Tokamak scenarios, internal transport barriers are now characterised in real time with a new criterion ρ^*_T; tailoring of the current profile with LHCD provides reliable access to a variety of q profiles, with significantly lowered access power for barrier formation; rational q surfaces appear to be associated with ITB formation; Alfven cascades are observed in RS plasmas, providing an identification of q profile evolution; plasmas with "current holes" were observed and explained by modelling. Transient high confinement Advanced Tokamak regimes with H89=3.3, β_N=2.4 and ITER relevant q<5 are achievable in reversed magnetic shear. Quasi-stationary internal transport barriers are developed with full non-inductive current drive, including ~50% bootstrap current. Record duration of ITBs was achieved, up to 11 s, approaching the resistive time. Pressure and current profiles of Advanced Tokamak regimes are controlled by a real time feedback system, in separate experiments. The erosion and co-deposition data base progressed significantly, in particular with a new quartz-microbalance diagnostic allowing shot by shot measurements of co-deposition.

1. Introduction

With its divertor configuration, plasma size, heating and current drive capabilities, Tritium and Beryllium capabilities, and diagnostic systems, the JET device can access a wide range of operating regimes in conditions closest to those of a burning plasma experiment. Prior to and during the design phase of ITER, JET produced major contributions to the ITER Physics Basis [1] used to extrapolate plasma performance to ITER. In the last two years, these capabilities were further exploited, focusing on issues critical to finalise the details of the ITER design and prepare its operation. This shaping capability has been extended toward plasma shaping very close to that of ITER, in particular with high triangularity, δ~0.5, achieved at up to 2.5 MA (higher current requires higher power than presently available for relevant experiments). This shaping capability has been further extended late in 2001, following the removal of dome and septum from the MarkII-GB divertor. Operating at or near the foreseen ITER plasma shape has proven essential, due to the strong effect of parameters like triangularity on ELMs, ELMy H-mode performance at high density and advanced modes. ITER operational scenarios can be optimised in a highly relevant and consistent range of parameters simultaneously achieved (δ, κ, q_{95}, as well as ρ^*, ν^* etc.). In addition, diagnostics capabilities have been improved, with new or upgraded systems commissioned in the last 2 years, such as correlation reflectometry, Electron Cyclotron Emission (ECE), quartz microbalance, improved Motional Stark Effect (MSE), shape controller upgrade, halo current diagnostics and pellet spectrometers. The real time control system has been developed, and proved to be successful in demonstrating the capability to control pressure or current profiles of plasmas with Internal Transport Barriers.

This overview paper presents only a selection of recent JET results, concentrating on advances in the two main operating regimes foreseen on ITER, the ELMy H-mode and Advanced Tokamak scenarios. New results on material migration and co-deposition are also presented. More details, as well as other results, can be found in accompanying presentations at this conference [2,3,4,5,6,7,8,9,10,11,12,13,14,15,16,17,18,19]

2. ELMy H-mode

One of the key scientific programmes conducted on JET is dedicated to further consolidating the ITER reference scenario, the ELMy H-mode [20,21]. ELM studies are presented in section 2.1, followed in section 2.2 by key MHD and fast particle issues, such as NTMs and α-simulation investigated in ELMy H-modes. Section 2.3 summarises performance achievements: high confinement at high density and high β.

2.1. Edge Localised Modes (ELMs)

Dedicated studies have investigated ELM size scaling [2], power loads at the divertor target [3], techniques for ELM amelioration and mitigation [4], MHD stability and characteristics of ELMs in Advanced Tokamak scenarios. The new expectations for Type I ELMs in ITER now span the tolerable range.

2.1.1. Scaling of ELMs with pedestal characteristics, ITER predictions

A high quality dataset of well-documented discharges in Type I ELMy H-mode indicates that ELM size is governed by plasma characteristics at the top of the pedestal, while ELM frequency is governed by inter-ELM transport [2]. The JET data also contributed to a revision for estimates of ITER tolerable ELMs [22,3].

Characterisation of the pedestal region in JET ELMy H-mode with Type I ELMs shows that typically the plasma pressure collapses in about the outer 15-20% of the outer plasma minor radius in a ~ 200 μs time-scale. Increasing the $n_{e,ped}$ decreases the relative drop in $T_{e,ped}$ (conductive ELM loss) but not in $n_{e,ped}$ (convective ELM losses). For some configurations Type I ELMs are identified, in which the ELM energy losses are purely convective [23]. New results at high δ in JET experiments have shown a break of the relation between Type I ELM frequency and size with increasing pedestal density, as illustrated in Fig. 1. At high $n_{e,ped}$ a decrease of f_{ELM} is observed together with a slight decrease of ΔW_{ELM}. This anomalous behaviour of the Type I ELM frequency is associated with an enhanced level of fluctuations in-between Type I ELMs with similar characteristics to those seen in Type II ELMs [24]. The anomalous ELM behaviour has been instrumental in demonstrating that the ELM energy loss is determined by the values of the pedestal plasma parameters while the ELM frequency is a consequence of the in-between ELM transport. An empirical correlation was found between the normalised Type I ELM energy loss (to the pedestal energy), $\Delta W_{ped}/W_{ped,}$ and the pedestal plasma collisionality, for a large range of plasma conditions, as shown in Fig. 2. Alternatively, the $\Delta W_{ped}/W_{ped}$ data is also well ordered by the ion transit time along the connection length, $\tau_{||ion}$, calculated with ion pedestal values. This could be related to the impedance for heat flux through the divertor target sheath during the ELM, and the connection of the pedestal plasma with the divertor target along ”broken” field lines [25].

Estimates of expected divertor lifetime in ITER have been reviewed and modified [22,3], as data from JET, other devices and material tests provided a more refined basis for modelling of acceptable ELM power load on target components. Marked on Fig. 2. are the present estimates of the acceptable ELM energy in ITER, assuming either 60% or 100% of plasma energy loss arrives at the target (50-80% observed at JET). The upper and lower values in

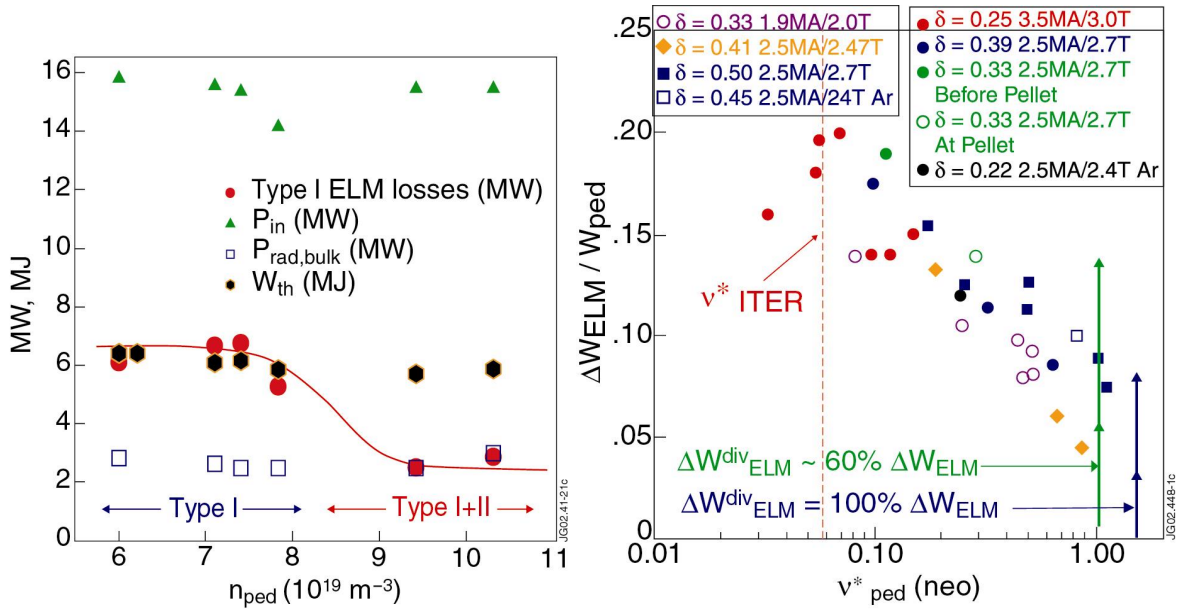

Fig. 1 Loss power balance of a gas scan. At highest pedestal density, average ELM losses are reduced, indicating an additional loss mechanism in between ELMs. Also, see Section 2.3.1.

Fig. 2 Scaling of Type I ELM size with pedestal collisionality.

each range originate from differences in the assumptions of ELM power deposition and ITER divertor target options [22].

2.1.2. Impurity seeding for ELM mitigation

ELM mitigation by impurity seeding has been demonstrated in JET [9,4]. With Ar, in Type I ELMy H-modes, the increase in edge radiated power leads to a reduced target peak heat load, measured by IR thermography of the divertor target plates. Ar seeding leads to a decrease of the ELM frequency and a reduction in $\Delta W_{ELM}/W_{ped}$, correlated with a change of the pedestal parameters, as was shown in Fig. 2.

2.1.3. MHD stability of the H-mode edge pedestal

The stability of H-mode edge pedestals has been analysed considering medium to large n kink/ballooning modes [26,24] and including stabilising diamagnetic effects [27]. In the second stable regime for infinite n ballooning modes, the medium-n ballooning modes set the actual limit on the pressure gradient: higher than 1st stability, but not second stable. Integrated transport/MHD modelling is being used to study the effect of edge density on plasma collisionality and therefore on bootstrap current and stability [5]. Study of ELM precursors and post-cursors and inter-ELM activity is on-going [28,6].

2.1.4. ELMs in AT scenarios

Controlling ELMs is important in Advanced Tokamak (AT) scenarios, as large Type I ELMs can destroy the ITB [29]. In typical AT discharges in JET, Type-III ELMs can be maintained at heating powers exceeding the threshold for the Type-III to Type-I ELM transition in H-mode by a factor of 2 [30]. This observation lead to a study of the effect of current ramps in high (ITER-relevant) triangularity discharges, showing that the edge stability is modified and type I ELMs can be suppressed in AT scenarios [7].

2.2. Key MHD issues in ELMy H-mode: NTMs, Sawteeth and α-physics effects

In ELMy H-mode discharges, core MHD can have an impact on confinement, which can, in turn, depend on kinetic effects.

TABLE I: PERFORMANCE ACHIEVEMENTS IN ELMY H-MODE IN JET

	High δ, high power #53299 (Type I-II)	High δ, Ar seeding #53550, Type I	ITER
$H_{98(y,2)}$	0.91	0.96	1.0
$\beta_{N,th}$	2.0	2.0	1.81
f_{GWD}	1.1	1.0	0.85
Z_{eff}	1.5	2.2	1.7
P_{rad}/P_{tot}	0.4	0.7	0.58
κ, δ	1.74, 0.48	1.7, 0.4	1.84, 0.5
q_{95}	3.2	3.1	3.0
τ_{pulse}/τ_E *	15	10	110

*Limited by technical constraints only.

In JET, it has long been known that MHD activity triggered by large sawteeth can reduce confinement. Notably, during the JET DT campaign, sawtooth control raised fusion power by 30% from a saturated value of 10 MW. This was obtained by delaying the sawtooth crash (fine-tuning the gas puff rate), and therefore avoiding confinement degradation. Recent modelling shows that fast particle stabilisation lead to larger sawteeth, triggering NTMs and reducing confinement in these fusion-relevant plasmas [31]. This lends credibility to α-simulation, discussed later in this section, where equivalent evolution is observed.

Concern about the effect of NTMs on confinement in ITER prompted a series of studies in JET on NTM stability, in ELMy H-mode plasmas [8,32]. An important result is that, for typical H-mode conditions in JET, the plasma is meta-stable to NTMs [33]– i.e. a sufficiently large perturbation will induce an NTM (usually m=3, n=2). Most commonly, the NTM seed perturbation is a sawtooth, suggesting the opportunity for NTM control via control of the sawtooth seed. Detailed scans have shown that current drive from 2nd harmonic ICCD, when located just inside the sawtooth inversion radius, causes small frequent sawteeth. In a seminal experiment, this sawtooth control has been exploited to raise the 3/2 NTM β-limit in JET discharges up to β_N=3.6 [34].

The ρ* scaling of the onset β_N value for the appearance of the NTM is important for prediction of NTM behaviour in ITER. The range of ρ* values has been extended to ~1.5 of ITER in JET by NTM seeding with long period sawteeth (mainly due to ICRH). The NTM onset β_N value for various devices is plotted in Fig. 3 vs. ρ* (derived from [35]), illustrating the importance of developing NTM control strategies for ITER

On-axis ion cyclotron resonance heating (ICRH) of neutral beam injected ^{4}He ions (3rd harmonic) produced a high-energy population of ^{4}He ions which simulate 3.5 MeV fusion-born alpha particles [36]. Strongest tails were created with highest energy ^{4}He seed beams, as expected. In these stationary plasmas, fast ^{4}He provided up to 80-90% of plasma heating. The successful acceleration of ^{4}He beam ions to the MeV energy range was confirmed by measurements of gamma ray emission from the reaction ^{9}Be(α,nγ)^{12}C [37] and excitation of Alfvén eigenmodes [38,10], and was consistent with the observed heating of the background electrons and sawtooth stabilisation, providing yet another example of the interconnection between the various physics events: fast particles stabilise sawteeth, which acquire large amplitude, trigger NTMs, and confinement is degraded [see 8]. This scheme can now be used in forthcoming JET campaigns with ^{4}He plasmas for dedicated alpha-particle studies.

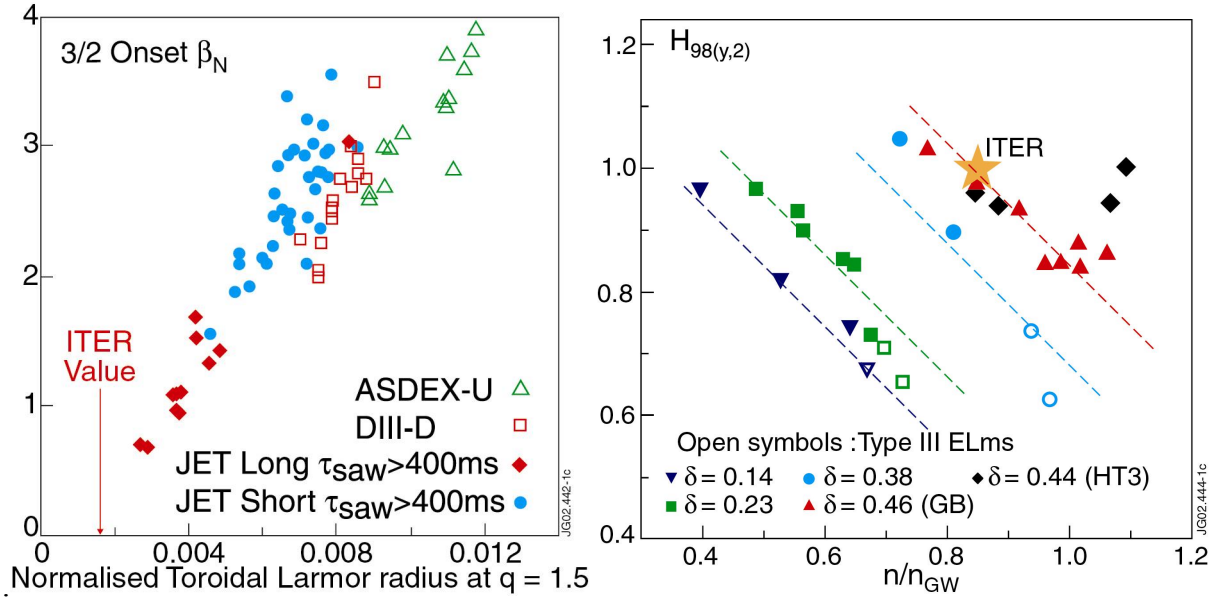

Fig. 3 Onset β_N for 3/2 NTM, as a function of $\rho^*(q=3/2)$, as defined in [35]

Fig. 4 H factor vs. Greenwald factor, as a function of triangularity, δ.

2.3. Integrated ELMy H-mode scenarios

High performance ELMy H-mode integrated scenarios have been achieved with various methods [20, 9], as displayed in Table I

2.3.1. High confinement at high density, achieved with high triangularity, high power

Experiments studying the beneficial effect of triangularity [24] and high heating power [39] on confinement have confirmed and extended earlier results, demonstrating high H factor at high density, see Table I. These discharges have single lower null, with ion grad B drift towards the X-point, standard q profile, NBI heating and gas fuelling. Significantly, the separatrix geometry was similar to that envisaged for the standard Q =10 operation in ITER, with average triangularity δ~0.45–0.5 and elongation κ ~1.75. Fig. 4 illustrates the beneficial effect of high triangularity on confinement at high density, up to the Greenwald density (n_{GR}).

In those high delta, high density, plasmas, a decrease of the Type I ELM frequency with density is observed, associated with high pedestal density: $n_{ped.} \geq 70\% n_{GR}$. The reduction of f_{ELM} is associated with high frequency fluctuations in the D_α emission (and enhanced D_α baseline level) in the inter-ELM period, accompanied by the appearance of a characteristic broadband MHD turbulence and by an increase of the density fluctuations in the pedestal region. This inter-ELM activity is also associated with high pedestal pressure and increased plasma power losses (See Section 2.1.1). The comparison with results from AUG [40] suggests that those high frequency D_α oscillations could be identified as Type II ELMs. Plasmas where Type I and Type II ELMs coexist are also observed in both AUG and JT-60U [41], when the critical parameters for the complete suppression of Type I ELMs are approached.

2.3.2. Impurity seeding

Stationary high performance phases (up to 12 τ_E) have been obtained with impurity seeding, simultaneously satisfying or exceeding the ITER Q=10 ELMy H-Mode requirements for $H_{989(y,2)}$, f_{GWD} and β_N [9], as shown in Table I. In low δ plasmas, with the X-point on the

septum, there is a pronounced peaking of the electron density profile. In high δ plasmas, the formation of a radiating belt inside the separatrix has been clearly established with high radiative power fractions up to 70%. Central impurity accumulation was avoided by application of ICRF heating, maintaining the safety factor on axis below 1, so sawteeth expelled impurities [42].

2.3.3. High confinement at high density, obtained by pellet injection

An optimized pellet sequence has been developed, consisting of a first phase where the density is increased (while allowing a small confinement loss) followed by a second phase minimizing the particle flux in order to maintain the density and to recover confinement. In this way, simultaneously $H_{98(y,2)} \sim 0.8$ with $\beta_N > 1.8$ and $f_{GWD} \sim 1$ have been reached, albeit not yet under stationary conditions. The plasma density profile shows a large peaking with $n/n_{ped} = 2$ and a decrease of Z_{eff} to about 1.7 is obtained at the highest densities reached [43].

2.3.4. Density peaking

Long time-scale density peaking has been observed in JET plasmas leading to densities exceeding the Greenwald value [44]. These neutral beam heated discharges are characterised by type-I ELMs and good energy confinement. The central density is limited by NTMs or by termination of the H-mode, preceded by loss of sawteeth. When these limiting factors are avoided (i. e. at intermediate power level and with optimisation of gas puffing) quasi-stationary high density plasmas with peaked density profiles are obtained. Whether the peaking is associated with an anomalous pinch is an issue still being investigated.

2.3.5. Scaling laws

The influence of peaking, triangularity and proximity to the Greenwald limit on energy confinement scaling has been investigated and has a minor effect on confinement predictions for ITER (<10% in τ_E) [45]. A set of experiments in He [46] (with a purity $C_{He}/C_D = 85\%$) added to our knowledge of the scaling of confinement with Z: $\tau_E \propto Z^{-0.59}$. The L-H threshold power in He plasmas shows the same B_t and n_e dependence as in D plasmas, but is 50% higher in absolute value.

A two term scaling law has been developed in the frame of the ITPA H-mode database working group. The best fit for an ELMy-H mode is compatible with an L-mode core and a pedestal confinement that depends sensitively on β. This finding is not compatible with strongly stiff profiles since in this case the central temperature is proportional to the pedestal height. The question of stiffness has been investigated on both experimental [11,17] and theoretical sides. ICRH modulation experiments with mode conversion in L mode show the existence of a threshold for electrons [12]. For ions evidence has been obtained from steady-state profiles in H mode [47]. In general a transport model based on a critical gradient gives a satisfactory prediction of confinement, but with a moderate stiffness factor. The global confinement time obtained with the values of instability threshold and stiffness factor found in JET is compatible with the ITPA two term scaling law.

2.4. Future plans, in ELMy H-mode regimes.

The plasmas shown in Table I demonstrate net progress towards the ITER targets, together with encouraging developments in ELM scaling. Extensions of ELMy H-mode studies to plasmas with higher currents, fields and heating powers and longer flat-top duration are planned. Plasmas with higher absolute densities and nearer to ρ^*_{ITER} can be developed, testing the limits of high performance regimes, enabling studies of Type I ELM scaling at low, ITER-like, collisionality, and of NTM scaling. New plasma configurations with ITER values of κ

and δ have already been developed and tested with current up to 2.5 MA. The estimated disruptive force implies that such plasmas can be explored, up to 4MA/4T, when more auxiliary power becomes available. NTM control techniques will be tested. Work on Type II ELM regimes will continue.

3. Advanced Tokamak Research on JET

The ultimate goal of Advanced Tokamak (AT) research is to provide steady-state operational regimes with possibly improved fusion performance. These modes are candidate for the steady-state operation of ITER [1]. Presently, AT research on JET is mainly focused on plasmas with internal transport barriers (ITBs) [48,7]. In section 3.1 experimental and modelling progress in ITB physics is reported. In section 3.2 the achievement of high performance and of long pulse ITB plasmas is presented. The demonstration of real-time control of pressure and current profiles is reported in section 3.3.

3.1. Internal Transport Barriers physics

A novel criterion for characterisation of ITBs: barrier formation and strength are operationally characterised in JET by $\rho^*_T = \rho_s/L_T$ (ρ_s: ion Larmor radius, at the ion sound speed, L_T: local T_e gradient length). Analysis of the JET ITB database and of a set of turbulence simulations led to the ITB onset criterion $\rho^*_T>0.014$ [13,49]. ρ^*_T can be computed in real time, characterising ITB formation and evolution (see Fig. 5), and providing an input for real time control (section 3.2).

LHCD aids current profile shaping: the coupling of the Lower Hybrid wave in all type of plasmas was greatly improved by puffing CD_4 near the launcher and matching the plasma shape [50, 51, 52]. Further optimisation led to dramatic increase in the availability of the LH system, with power levels in the 3-4 MW range routinely coupled to high power 15-20 MW plasmas. LHCD became an efficient tool to access ITBs and control them through off-axis current drive. Off-axis co-LHCD in the prelude phase (current ramp up) of JET plasmas easily and reliably provides magnetic shear reversal, providing target plasmas with appropriate current profile often exhibiting an early "electron barrier". The current profile is then "frozen" by the application of heating (NBI, ICRH) and ITBs develop.

Current Holes: the Motional Stark effect measurements (MSE) of the poloidal magnetic field [53] showed plasmas with essentially no toroidal current density in the core of JET ITB discharges (a region of up to 20 cm diameter). These where explained as an effect of the non-inductive, off-axis co-LHCD, which induces a negative voltage in the plasma core. Similar "current holes" were observed in JT-60 but driven solely by NBCD and bootstrap [54,55]. The core current density does not appear to become negative (error bars on plasma core current are ±10-20 kA), although current diffusion calculations indicate that there is sufficient core negative voltage to cause current reversal [56]. This apparent clamping of the core current density near zero is consistent with n=0 reconnection events redistributing the core current soon after it goes negative, as shown in reduced resistive MHD simulations in cylindrical geometry [57] and in 2-D nonlinear resistive MHD simulations in toroidal geometry [58].

Rational q surfaces and transport barriers: a careful analysis of both low shear and reversed shear ITBs demonstrates the key role played by the q-profile itself and, in particular, by the presence of *q = 1, 2 or 3* surfaces in the plasma edge and core [14]. The formation of

low shear ITBs is well correlated with the occurrence of rational edge-q values [59]. With reversed magnetic shear, experimental evidence (including Alfvén cascades, see below) also

suggests a link between the appearance/development of an ITB and rational q surfaces (e.g. q_{min}=2) entering the plasma core [60], as shown in Fig. 5. Possible explanations are put forward: coupling of MHD modes located at rational q surfaces can generate stabilising velocity shear; gaps in the density of rational surfaces near rational q surfaces can have a stabilising effect on low wave number ITG/TEM turbulence [13,14].

Alfvén Cascades: in reversed shear ITB plasmas cascades of Alfvén modes sweeping upwards in frequency have been observed, as previously in JT60-U [[61], [62]Ref: JT-60, JET]. Each cascade consists of many modes, driven by ICRF-accelerated ions. These Alfvén cascades have been interpreted in terms of a novel-type of Energetic Particle Mode [63,64,65] localised at the point where $q(r)$ has a minimum. The frequency of the Eigenmode tracks the evolution of q_{min}, which opens the possibility of Alfvén spectroscopy measurement of $q(r, t)$ [66]. Indeed Alfvén cascades are now used as an auxiliary rational q measurement on JET, as well as identifiers of shear reversal. The intrinsic interest of TAEs and cascades in potential steady state burning plasmas is being explored by various groups [10,38,67]

3.2. High Performance and Steady State ITBs

High performance ITBs: in transient states, reversed shear high performance plasmas with wide ITBs (r/a~0.6) have been achieved. The stronger ITBs are triggered when q_{min} reaches 2, and within experimental uncertainties, ITBs are detected simultaneously, and at the same location, in electron and ion temperatures (T_e and T_i), density and plasma rotation profiles.

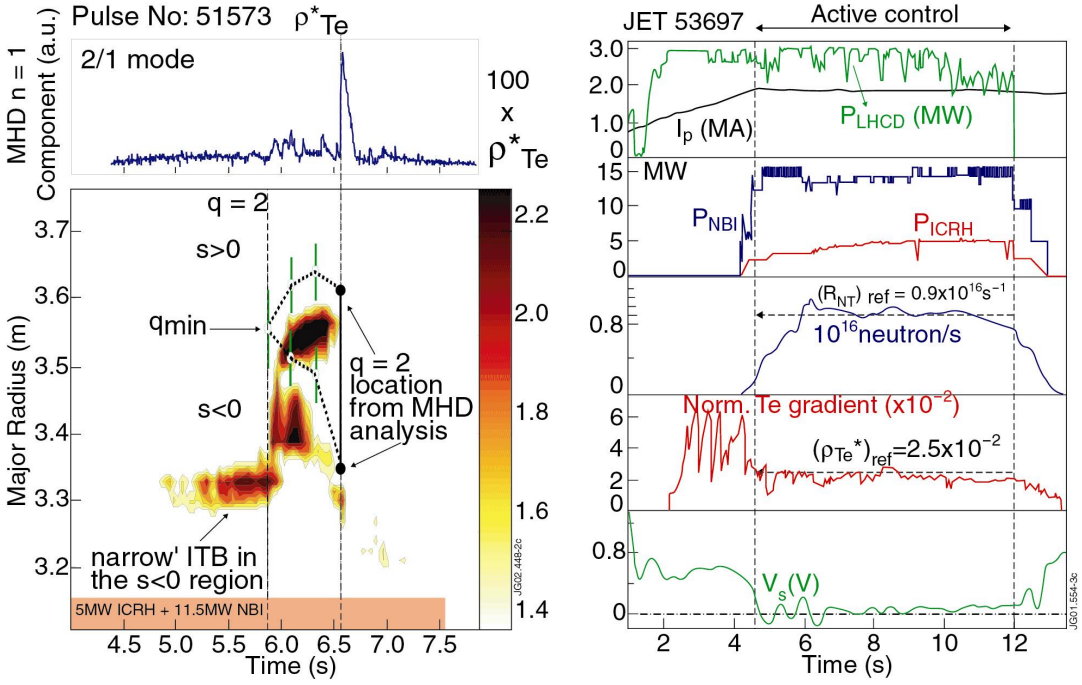

Fig. 5 Plot of ITB criterion versus time and plasma radius. When q_{min} crosses 2 the barrier is broadened (radius increased by ~30 cm) and two barriers are follow the evolution of the q=2 surfaces. The time when q_{min} crosses two is confirmed from the excitation of Alfvén cascades.

Fig. 6 Time evolution of the main parameters of a discharge with combined ρ_{Te} and R_{NT} feedback control using ICRH and NBI powers (#53697, B_t=3.4 T, I_p=1.8 MA)*

With reversed magnetic shear, the access power is low, and β_N and the fusion yield for given input power is high. The parameters of one of the highest performance ITB plasmas are shown in Table II [68]. Notably β_N= 2.4, and q_{95}=4.9, with 2.5 MA of plasma current. The current profile is broad, maximum available heating (4MW ICRH and 17MW NBI) was used. Density peaking leads to impurity accumulation [15]. In this case, the transient high performance phase ends with a large ELM followed by a disruption. (global pressure n=1 kink mode instability).

Record long pulse ITBs: by tailoring the internal plasma profiles to keep confinement and stability under control, the duration of ion ITBs could be prolonged to up to 7.5 seconds of plasma flattop, corresponding to $27\times\tau_E$ [69,70,7]. The discharge parameters are presented in Table II. This is a record duration for an ion ITB in JET. In this case, an electron ITB was formed during the ramp-up, and had an overall duration of $37\times\tau_E$. In this long duration ITB discharge, the fusion performance is lower than in transient cases (see Table II), while the non-inductive current fraction was much larger. Radiative or MHD core collapses of the ITB are observed: plasma pressure, toroidal rotation and electric fields collapse on a fast time scale. Surprisingly, the ITB is reformed immediately after the collapses. The implication, supported by turbulence simulation studies, is that as long as the q profile is not affected by the collapses, it remains favourable for ITB formation, and the ITB will re-form. At a slightly lower plasma current of 1.8 MA full non-inductive current drive was realised [7].

Development of real time control tools: achieving steady-state real-time control of ITBs requires diagnostics allowing a reliable characterisation of the key parameters and appropriate actuators. The new ITB criterion ρ^*_T is used to characterise ITBs in real time, interfero-polarimetry provides a q profile measurement and the neutron production rate characterises ITB plasma performance. All these real time measurements are used as input values for the new Real Time Control System. The main actuators used are the three heating systems, LHCD, NB and ICRH, all having different (but coupled) effects on ITB behaviour.

TABLE II: ADVANCED TOKAMAK SCENARIO DEVELOPMENT ON JET

JET ITB	High Performance *(pulse 51976, t=6.8s, Ip = 2.5MA, Bt =3.45T)*	Long pulse *(pulse 53521, t=10s, Ip = 2.0MA, Bt =3.45T)*	ITER Target *as derived from ITER design basis1*
H_H (IPB98y-2)(thermal)	1.9	1	> 1.5
$H_{ITER\ 89\ L\text{-}P}$	3.3	2.1	
β_N	2.4	1.7	> 3.0
$I_{Non\text{-}Inductive}/I_p$	55%	90%	100%
I_{boot}/I_p	40%	50%	> 60%
q_{95}	4.9	5.5	4.5
P_{rad}/P_{tot}	15%	23%	75%
n_{io}/n_{eo}	0.7 =(3.85/5.5) 10^{19}	0.65 = (4/6.2) 10^{19}	
$\tau/\tau_{conf.}$, $\tau/\tau_{resistive}$ (*)	2, ~0.1	27, ~1	
n_{eo}/n_{GW}, n_{el}/n_{GW}	0.65, 0.35	0.8, 0.5	n_{el}/n_{GW} > 0.6
Edge	Type III ELMs	Type III ELMs	Mild ELMs

(*) τ = duration of ITB regime; $\tau_{resistive}$ is calculated at the ITB foot-point

Demonstration: real time control of pressure and current profiles. The above-mentioned tools have been used in a first series of real time feedback demonstrations, based on the largely non-inductive long pulse discharges described above. Pressure profile and barrier strength control is illustrated in Fig. 6. Having established an appropriate target current profile, reliable and reproducible ITB operation is achieved by controlling the neutron yield by NBI heating, while ICRH is used to act on the maximum electron temperature gradient directly [71]. The LHCD is maintained in a pre-programmed way to provide a broad q-profile ensuring core confinement and stability. During the control phase, the plasma parameters of the discharge are fairly stationary with mild and continuous ELM activity. Thanks to the real time control of the ITB characteristics, the improved confinement state is maintained in a reproducible and stationary manner, e.g. avoiding the occurrence of core collapses. In separate experiments, it has also been shown that the LHCD feedback can be used in conjunction with real time measurement of q to maintain a desired q profile fixed for several seconds [72]. These demonstrations open the path toward fully controlled steady state Advanced Tokamak plasmas.

3.3. The future: high performance in steady state.

The plasmas shown in Table II demonstrate net progress towards the ITER target of steady state plasmas. To achieve steady-state high fusion performance, the current and pressure profile must be controlled simultaneously, the density must approach the Greenwald value, impurity accumulation must be avoided or controlled, bootstrap must be high (high pressure and high power), and edge radiation must be increased, or the SOL broadened. Operation in ITER-like triangularity, made possible by the recent divertor modification, contributes to make the results more directly applicable to ITER prediction.

4. Erosion and co-deposition

Erosion and deposition constitute one of the key topics in preparation of ITER operation, as they influence the lifetime of divertor tiles and other plasma facing components (PFCs), and the in-vessel tritium inventory. JET experiments provide a database against which models can be tested [16].

Tiles from the MkII-GB divertor were removed during the 2001 shutdown. Analysis of tile surfaces [73,74] confirmed previous observations: the inner divertor is subject to net deposition of plasma impurities (and retention of D and T). No comparable net erosion is observed in the outer divertor, implying that the primary source of eroded impurities are main chamber PFCs. This analysis shows that deposited films are enriched in Be and other metals, while carbon is chemically eroded and transported to shadowed regions of the inner divertor [75].

Measurements made during the 2001 He campaign differentiate physical and chemical sputtering. The main source of C in L-mode plasmas appears to be chemical sputtering at the inner divertor and main chamber wall. In ELMy H-mode the situation is less clear, but the data points to a strong physically sputtered C-source from the main chamber and outer divertor [76], while chemical erosion dominates in the inner divertor in all cases.

In ohmic plasmas, atoms of ^{13}C were injected into the top of the JET vessel, at the end of the MarkIIGB operation (divertor temperature had been lowered to ~100ºC). About one-half of the injected ^{13}C is found on the inner divertor tiles intersected by the SOL, and a negligible amount is found at the outer divertor [73], consistent with previous findings. No ^{13}C was found on shadowed regions of the tiles, where otherwise thick carbon layers have built up in the past [75]. This may indicate a reduced long range carbon transport due to reduced

chemical erosion at lower operating temperatures [74], but it might be also connected with the special (ohmic) plasma operating conditions [16].

First measurements of pulse resolved growth of carbon layers near the inner louver situated inside the divertor pumping throat have been made with a newly developed quartz micro-balance (QMB). This diagnostic is capable of measuring deposited layers at the mono-atomic layer level. The average growth rate (deposited carbon atom on louver divided by total ion flux into the inner divertor) was found to be of order $2\ 10^{-4}$ C/ion [77], 200 times smaller than previously estimated from the DT campaign. A thorough investigation is underway to explain these differences.

5. Tritium Technology R&D

Special detritiation techniques are developed for components replaced during operations to allow waste disposal under economically sound and environmentally safe conditions [78,79,80]. Water detritiation techniques are also being developed: laboratory size plants with liquid phase catalytic exchange (LPCE) column have been built to test the performance of various packing materials and catalysts and to determine mass transfer for D and T between water and gas [81,82]. Design studies of a water detritiation plant at JET are on going [83]. During the 2001 shutdown flakes from the sub-divertor region of the tokamak were collected remotely to help reconcile the tritium balance at JET [84,85].

6. Disruption Studies

Thermal loads: The current ITER assumption for disruptions is that the energy from the thermal quench is deposited in the divertor. Recent analysis shows that only a few percent of the thermal and thermal plus magnetic energy can be accounted for in the JET divertor [86] and it is spread rather uniformly. If the same applies in ITER, then the energy density within the divertor would be below the level at which carbon ablation or tungsten melt layer formation are expected [3].

VDEs: Modelling of vertical displacement events (VDEs) in JET has improved, with a better representation of eddy currents in the vacuum vessel. Now there is good agreement between theoretical predictions of VDE evolution and experimental results: growth rates have been estimated within an accuracy of 5% for plasmas with a growth time longer than 2 ms [87,88].

Runaways: Regions of parameter space have been identified in which disruptions lead to runaway generation in JET [89]. They appear when q_{95} and B_t exceed threshold values (ie B_t above ~2T), in good agreement with observations on JT60-U [90]. The delay in runaway generation following the temperature collapse is found to be caused by the very high density generated by the disruption. It can be concluded that avalanching is probably the dominant process in runaway electron formation in JET and therefore runaway control techniques can be tested for ITER. Initial tests in this regime have shown that it is possible to quench the plasma with large helium puffs without producing runaways.

7. Future plans

The present plan of exploitation of the JET facilities for the years 2003 and 2004 foresees experimental campaigns in 2003 and until February 2004. In 2003, two experimental campaigns are dedicated to further develop ELMy H-mode and ITB modes, one campaign to Trace Tritium Experiments in deuterium plasmas, one to reversed magnetic field experiments in deuterium. The last campaigns before the 2004 shutdown is reserved for hydrogen and

helium plasmas in particular to provide data in preparation of ITER non-activation phase. From March 2004 a long shut down period is planned for installation of enhancements.

The Trace Tritium Experiment (TTE) shall take full advantage of the unique Tritium handling capability of JET. The TTE is planned with ~1.5 % Tritium in Deuterium plasmas. Transport of Tritium particles will be investigated with neutron and γ emission diagnostics. A study of particle (fuel ion, Helium and impurities) transport is planned in ELMy H-modes and AT scenarios, continuing and greatly extending the work initiated in the previous Trace Tritium Experiment [91]. In particular, a study of fuel ion transport has never been done in AT scenarios, and would be important in preparation of future DT AT operation on JET or/and ITER. The use of trace tritium also offers an opportunity to study aspects of ICRF heating schemes and Fast Particle Physics (fast ions in current hole scenarios). The TTE has the added benefit of exercising and maintaining technical expertise on tritium handling in a tokamak environment. It finally permits relevant testing of new systems foreseen to find application on ITER, such as detritiation catalysts, and an ITER-design cryo-panel [92,93].

In the 2004 shutdown it is planned to install a new in-port ICRF antenna. The aims are to validate key elements of the ITER ICRF design (such as ELM-tolerant operation at high power density), and to deliver an additional 7 MW of heating power, allowing higher performance operation closer to ITER plasma parameters. By then, planned diagnostic upgrades include CXRS core and edge, magnetics, bolometry, neutron spectrometry, microwave waveguides, divertor diagnostics. New diagnostics to be installed include a high resolution Thomson Scattering System, TAE active antenna system, wide angle Infra-Red view, Halo Sensors, Lost α detectors and a comprehensive system of erosion/re-deposition diagnostics.

8. Conclusions

JET continues to provide vital contributions to understanding of tokamak physics, scaling predictions for ITER, further development of ITER operating scenarios and testing of ITER relevant systems, such as heating and current drive, diagnostics and Tritium technologies.

9. Acknowledgements

This work was performed under EFDA, by JET EFDA contributors, listed in Annex I. The JET EFDA Leader would like to acknowledge the work of all JET EFDA contributors, specially the JET Task Force Leaders during this period: A. Bécoulet., P. Buratti, F. Crisanti, X. Garbet, C.-R. Grisolia, T. Hender, A. Kallenbach, R. Laesser, X. Litaudon, S. Günter, P. Mantica, G. Matthews, P. Monier-Garbet, A. Murari, J.-M. Noterdaeme, J. Ongena, R.-D. Penzhorn, V. Philipps, S. Pinches, J. Sanchez, O. Sauter, D. Stork, W. Suttrop, A. Tuccillo, H. Weisen, R. Wolf. Equally, the JET EFDA Leader would like to express his thanks to all staff working under the auspices of the JET Operation Contract, whose hard work and knowledge made experimental operation possible, and to the EURATOM/UKAEA Fusion Association. Special contributions to this paper were made by M. Bécoulet, D. Brennan, G. Buceti, D. Campbell, S. Ciattaglia, P. Coad, E. Joffrin, N. Hawkes, G. Huysmans, V. Krivenski, P. J. Lomas, A. Loarte, M. Mantsinen, D. Moreau, F. Nave, R. Pitts, J. Rapp, V. Riccardo, G. Saibene, R. Sartori, B. Stratton, D. Testa, M. Valovic, K.-D. Zastrow, and by Emilia R. Solano, who helped write the paper.

[1] ITER Physics Basis, Nucl. Fusion, **29** (1999) 2368.
[2] LOARTE, A., "Type I ELM energy and particle losses in JET ELMy H-modes and implications for ITER", these proceedings (paper EX/P1-08)
[3] MATTHEWS, G.F.,"Steady state and transient power loads in JET", these proceedings (paper EX/D1-1)
[4] RAPP, J., "Reduction of divertor heat load in JET ELMy H-modes using impurity seeding techniques", these proceedings (paper EX/P1-09)
[5] PARAIL, V., "Integrated Modelling of JET H-mode Plasmas with type-I ELMs", these proceedings (paper TH/P3-08)
[6] KOSLOWSKI, H.R., "Observation of Pre- and Postcursor Modes of Types I ELMs on JET", these proceedings (paper EX/P1-14)
[7] LITAUDON, X., "Progress towards steady state operation and real time control of internal transport barriers in JET", these proceedings (paper EX/C3-4)
[8] HENDER, T., "Sawtooth, Neo-Classical Tearing Mode and Error Field Studies in JET", these proceedings (paper EX/S1-2)
[9] ONGENA, J., "Towards the realization on JET of an integrated H-Mode scenario for ITER", these proceedings (paper EX/C2-4)
[10] TESTA, D., "Experimental Study of the Stability of Alfven Eigenmodes on JET", these proceedings (paper EX/P1-17)
[11] NOTERDAEME, J.-M., "Heating, current drive and energetic particles studies on JET in preparation of ITER operation", these proceedings (paper EX/W-1)
[12] MANTICA, P., "Transient Heat Transport Studies in JET Conventional and Advanced Tokamak Plasmas", these proceedings (paper EX/P1-04)
[13] GARBET, X., "Micro-stability and Transport Studies of Internal Barriers in JET", these proceedings (paper TH/2-1)
[14] JOFFRIN, E., "Internal Transport Barrier triggering by rational magnetic flux surfaces", these proceedings (paper EX/P1-13)
[15] DUX, R., "Impurity transport in internal barrier discharges on JET", these proceedings (paper EX/C3-5Ra)
[16] PHILIPPS, V., "Recent results on long term fuel retention in JET and TEXTOR and predictions for ITER", these proceedings (paper EX/P5-08)
[17] SUTTROP, W., "Parameter similarity studies in JET, ASDEX Upgrade and ALCATOR C-Mod", these proceedings (paper EX/P5-07)
[18] HIDALGO, C., "Experimental evidence of fluctuations and flows near marginal stability in the plasma boundary region in fusion plasmas", these proceedings (paper EX/C4-4)
[19] CASTALDO, C., et. al., "Transport barriers produced in JET discharges by ion Bernstein waves", post-deadline paper, these proceedings.
[20] Special issue on "ELMy H-Mode Research on the JET Facility under EFDA during the 2000-2001 Experimental Campaign", Plasma Phys. Control. Fusion **44** No.9 (2002)
[21] SUTTROP, W., Phys. Plasmas, **9** (2002) 2103
[22] FEDERICI, G., et al., Proc. of 15th Int. Conf. on Plasma Surface Interactions in Controlled Fusion Devices, May 27-31, 2002, Gifu, Japan, to be published in JNM.
[23] LOARTE, A., et al., ibid., PPCF, 44, No.9, p.1815-1844
[24] SAIBENE, G., ibid., PPCF, 44, No.9, p.1769-1799
[25] JANESCHITZ, G., et al., Jour. Nucl. Mat. **290-293** (2001) 1.
[26] HUYSMANS, G.T.A., “Overview of MHD stability in edge transport barriers”, presented at the 9th European Fusion Physics Workshop 2001, Saariselka, Finland, 2001.
[27] HUYSMANS, G.T.A., et al., Phys. Plasmas **8** (2001) 4292
[28] PEREZ, C. et al., “Type-I ELM Precursor Modes in JET”, submitted to Nucl. Fusion.

[29] SÖLDNER, F.X., et al., Plasma Phys. Control. Fusion **39** (1997) B353
[30] BÉCOULET, M., et al., Plasma Phys. Control. Fusion **44** 2002 A103
[31] NAVE, M.F.F., et al., Nucl. Fusion **42** (2002) 2
[32] GŰENTER, S.. et al., Phys. Rev. Lett. **8**7, 275001 (2001),
[33] SAUTER, O., Plasma Phys. Control. Fusion **44** (2002), p. 1999.
[34] SAUTER, O. et al, Phys. Rev. Lett., **88** (2002) 105001
[35] LAHAYE, R. J., Phys. Plasmas **7**, 3349 (2000)
[36] MANTSINEN, M., et al., Phys. Rev. Letters **88** (2002) 105002-1.
[37] KIPTILY, V.G., et al., Nucl.Fusion **42** (2002) 999.
[38] JAUN, A., et al., "Collective modes and Fast Particle Confinement in ITER", these proceedings.
[39] SARTORI et al., Plasma Phys. Control. Fusion **44** (2002) 1801
[40] STOBER J. et al., Nucl. Fusion **41** (2001) 1123
[41]KAMADA, Y. and the JT60-U team, Nucl. Fusion **41** (2001) 1311
[42] NAVE, F. et al., "Control of Impurity Accumulation in JET Radiative Mantle Discharges", submitted to Nucl. Fusion
[43] LANG, P.T. et al., Nucl. Fusion **42** (2002) 388.
[44] VALOVIC, M., et al., Plasma Phys. Control. Fusion **44** (2002) 1911
[45] CORDEY, G., Plasma Phys. Control. Fusion, **44** (2002) 1929
[46] McDonald, D., in preparation.
[47] WOLF, R.C. et al., "Characterisation of ion heat conduction in JET and ASDEX-Upgrade plasmas with and without internal transport barriers", submitted to Plasma Physics and Controlled Fusion.
[48] Special issue on *"Advanced tokamak research in EFDA-JET during the 2000-2001 experimental campaigns"* 2002 Plasma Phys. Control. Fusion **44** 1031
[49] TRESSET, G., et al., Nucl. Fusion **42** (2002) 520
[50] MAILLOUX, J. et al., Phys. Plasmas **9** (2002) 2156
[51] PERICOLI, V. et al., *Radio Frequency Power in Plasmas,* (14th Topical Conf., Oxnard, CA, 2001), Vol. 595, AIP (2001) 245-248, submitted to Phys. of Plasmas.
[52] PERICOLI V., et al., ''Study and optimisation of lower hybrid waves coupling in advanced scenarios plasmas in JET'', submitted to Physics of Plasmas (2002)
[53] HAWKES, N.C., et al., Phys. Rev. Lett. **87** (2001) 115001-1.
[54] FUJITA, T., Phys. Rev. Lett. **87** (2001) 245001.
[55] MIURA, Y., these proceedings (paper EX/C3-1Ra)
[56] TALA, T.J.J., et al., Plasma Phys. Control. Fusion **4**3 (2001) 507
[57] HUYSMANS, G.T.A. et al., Phys. Rev. Lett. **87** (2001) 245002-1.
[58] STRATTON, B.C. et al., Plasma Phys. Control. Fusion **44** (2002) 1127
[59] JOFFRIN, E. et al., Nucl. Fusion **42** (2002) 235
[60] JOFFRIN, E. et al., Plasma Phys. Control. Fusion **44** (2002) 1739
[61] KIMURA, H. et al., Nuclear Fusion **38** (1998)1303
[62] SHARAPOV, S. E., et al., Phys. Lett. A 289 (2001) 127
[63] SHARAPOV, S.E. et al., Phys. Plasmas 9, 2027 (2002)
[64] ZONCA, F., "Energetic Particle Mode Stability in Tokamaks with Hollow q –profiles", submitted to Phys. Plas.
[65] BERK, H. L. et al., Phys. Rev. Lett. **87** (2001) 185002
[66] A. Fasoli et. al., PPCF, to appear 2002
[67] BREIZMAN, B.N., et al., "Alfvėn Eigenmodes in Shear Reversed Plasmas", these proceedings (paper TH/4-3)
[68] CHALLIS, C.D. et al., Plasma Phys. Control. Fusion **44** (2002) 1031

[69] CRISANTI F. et al., Phys. Rev. Lett. **88** (2002) 145004-1
[70] LITAUDON, X. et al., Plasma Phys. Control. Fusion **44 (**2002) 1057
[71] MAZON, D. et al., Plasma Phys. Control. Fusion **44 (**2002) 1087
[72] MAZON, D. et al., Proc. of 29th Eur. Phys. Conf., Montreux (EPS)
[73] LIKKONEN, J., et al., Proc. of 22nd Symposium on Fusion Technology (SOFT), Helsinki, Sept. 2002
[74] COAD, J.P. et al, Proc. of 15th PSI, Gifu, Japan, to be published in J. Nucl. Materials.
[75] COAD, J. P., et al., J Nucl. Materials 290-293 (2001) 224
[76] PITTS, R., et al., ibid., 15th PSI, Gifu, 2002, to be published in J. Nucl. Materials.
[77] ESSER, H. G., ibid., 22nd SOFT, Helsinki, 2002.
[78] BELL, A.C. et al., Fusion Science and Technology **41** (2002) 626
[79] ROSANVALLON, S. et al., Fusion Science and Technology **41** (2002) 695.
[80 PEREVEZENTSEV, A., et al., Fusion Science and Technology **41** (2002) 706.
[81] CRISTESCU, I. et al., "Simultaneous tritium and deuterium transfer in a water detritiation CECE Facility at TLK", Proc. 22nd SOFT, Helsinki, Sept. 2002
[82] PEREVEZENTSEV, A. et al., Fusion Science and Technology **41** (2002) 1107
[83]PEREVEZENTSEV, A. et al., Fusion Eng. Design **00** (2002) 1-5.
[84] PEREVEZENTSEV, A. et al.,Fusion Science and Technology **41** (2002) 821.
[85] COAD, J.P., et al, J. Nucl. Materials **290-293** (2002) 224.
[86] RICCARDO, V., et al., Plasma Phys. Contr. Fusion **44** (2002) 905-929
[87] ALBANESE R., et al., Nucl. Fusion, **38** (1998) 723
[88] ALBANESE, R., et al, submitted to Nucl. Fus., 2002.
[89] GILL, R. D., et al, "Behaviour of disruption generated runaways in JET", accepted for publication in Nuclear Fusion (2002).
[90] YOSHINO, R., et al, Y., Nuclear Fusion **39** (1999) 151
[91] JET TEAM, presented by ZASTROW, K.-D., Nucl Fus **39** (1999) 1891
[92] BRENNAN, D.P., Fusion Science and Technology, **41** (2002) 578
[93] DAY, CHR., et al., "A large scale cryopanel test arrangement for tritium pumping", Proc. 22nd SOFT, Helsinki, Sept. 2002

Annex 1: JET EFDA Contributors

Agarici M[2], Akhter H.[15], Albanese R. [5], Alberti S.[12], Allfrey S.[12], Alper B.[15], Alves D. [9], Amarante J.[23], Amerongen F.V. [6], Andrew P.[15], Andrew Y.[15], Ane J.M.[2], Angioni C.[12], Apruzzese G. [5], Artaserse G. [5], Ascasibar E.[3], Axton M.[15], Baciero A. [3], Badarelli M. [5], Baeumel [8], Balbin R. [3], Balme S.[2], Barana O. [5], Baranov Y.[15], Barbato E. [5], Barker P.[15], Barnsley R.[15], Bayetti P.[1-2], Baylor L.[19], Beaumont B.[2], Beaumont P.[15], Becoulet A.[2], Becoulet M.[2], Bekris M. [7], Beldishevski M.[15], Bell A.C.[15], Bennet P.[15], Bennett M.[15], Berger-By G.[2], Bernabei S.[18], Bertalot L. [5], Bertrand B.[2], Beurskens M. [6], Bibet[2], Bickley A.[15], Bigi M.[15], Bilato R. [8], Bird J.[15], Blackman T.[15], Blanchard P.[12], Blum J.[27], Bolzonella T. [5], Bondeson A.[10], Bongers W. [6], Bongers W.A.[6], Bonheure G[23], Bonnin X. [8], Borass K. [8], Borba D.[1-9], Bosak K.[27], Bosia G.[17], Bosia Pino[2], Bracco G. [5], Bradshaw J.[15], Bremond S.[2], Brennan P.D.[15], Brezinsek S. [7], Brichero B.[23], Bright M.D.J.[15], Briscoe F.[15], Brix M. [7], Brolatti G. [5], Brown D P D[15], Bruggeman A.[23], Bruschi A. [5], Bryan S.[15], Brzozowski J.[10], Bucalossi J.[2], Buckley M.A.[15], Budd T.[15], Budny R.[18], Buratti P. [5], Butcher P.[15], Buttery R.[15], Calabro' G. [5], Caldwel-Nicholas C.J. [7], Campbell D.[16], Campling D.C.[15], Cannas B. [5], Capel A.J[15], Card P.J[15], Carman P.[15], Castaldo C. [5], Cecil F. Edward[28], Cesario R. [5], Challis C.[15], Chankin A.[15], Chappuis Ph.[2], Charlet M.[15], Charreau J-M.[2], Cheron C.[2], Child D.[15], Chitarin G. [5],Ciattaglia S.[1-5], Cirant S. [5], Ciric D.[15], Clarke R.[15], Clay R.[15], Coad P.A.[15], Coates P.[15], Coccorese V. [5], Cocilovo V. [5], Coda S.[12], Coelho R. [9], Coffey I.[15], Coletti A. [5], Collins S.[15], Conboy J.[15], Conroy S.[10], Conway G. [8], Cooper S.R.[15], Cordey G.[15], Corre Y.[10], Corrigan G.[15], Cortes S. [9], Coster D. [8], Counsell G.[15], Cox M.[15], Cox S.J.[15], Cramp S.[15], Crescenzi C. [5], Crisanti F. [5], Cristescu I.[26], Crowley B. [4], Cruz N. [9], Cupido L. [9], Cusack R.[15], Da Silva Aresta Belo P. [9], Dailey S.[15], Damiani C. [5], Darrow D.[15], David O[2], Davies N.[15], Davis J.J.[15], Day C.[14], De Angelis R. [5], De Antonis P.[15], De Baar M. [6], De Barbieri O.[16], De Benedetti M. [5], Degli Agostini F. [5],De la Luna E. , De Vries P. [6], DeGrassie J.[20], Denyer R.F.[15], Dines A.[15], Dobbing J.A.[15], Doceul L.[2], Doncel J.[1-3], Donne A. [6], Donne T. [6], Dorling S.E.[15], Doyle P.[15], Drozdov V.[15], Dumbrajs O.[13], Dumortier P.[23], Durocher A.[2], Durodié F.[23], Duval B.[12], Dux R. [8], Edlington T.[15], Edwards A.M.[15], Edwards D.[15], Edwards P.[15], Eich T. [8], Ekedahl A.[2], Elbeze D.[2], Ellingboe B. [4], Ellis R.[18], Elsmore C.G.[15], Elzendoorn B. [6], Elzendoorn B.S.Q.[6], Erents K.[15], Ericsson G.[10], Eriksson L.[2], Esposito B. [5], Esser H.G [7], Estrada T. [3], Evrard M.[23], Ewart C.[15], Fanthome J[15], Farthing J.W. , Fasel D.[12], Fasoli A.[12], Felton R.[15], Fenzi C.[2], Fernandes H. [9], Fernandez A. [3], Ferreira J. [9], Fessey John[15], Figueiredo A. [9] P. [5], Finburg P.[15], Fink J. [8], Finken K-H. [7], Fiorentin[15], Fischer U. [7], Fleming C.[15], Formisano A. [5],Forrest R.[15], Franel B.[2], Franklin A.[15], Franzen P. [8], Fricconneeu J.P.[2], Frigione D. [5], Fuchs C. [8], Fukuda T.[22], Fullard K.[15], Fundamenski W.[15], Gabriel F.[2], Gaffert J. [8], Galutschek E.[11], Gans Timo [4], Garbet X.[2], Garcia-Cortes I. [3], Garzotti L. [5], Gauthier E.[2], Gedney J.[15], Geier A. [8], Gentile C.[18], Gerasimov S.[15], Ghendrih P.[2], Giannella R.[2], Gill R.D.[15], Gimblett C.[15], Giovannozzi E. [5], Giroud C. [6], Godden J[15], Goff J.[15], Gohil P.[20], Gondhalekar A.[15], Goniche M.[2], Goodyear A.[15], Gorelenkov G.[18], Gorini G. [5], Gormezano C. [5], Goulding R.[19], Gowers C.[15], Graham M.E.[15], Grando Luca [5], Granucci G. [5], Graswinckel M.[6], Graswinckel Martijn [6], Green J.A.[15], Green N.[15], Griph F.S.[15], Griph S.[15], Grisolia C.[2], Grosman A[2], Grosso G. [5], Gruenhagen S. [7], Gryaznevich M.[15], Gude A. [8], Guenter S. [8], Guenther K.[15], Guérin C.[2], Gugla M. [7], Guirlet R.[2], Gunn J.[2], Haas G. [8], Hackett L.[15], Hacquin S. [9], Hallworth-Cook S.[15], Handley R.[15], Harling J.D.W.[15], Harrison J.[15], Hartmann D. [8], Hatae T.[22], Hawkes N.[15], Hay J.[15], Hayward I.[15], Heesterman P.[15], Heikkinen J.[13], Heinemann B. [8], Hellermann Manfred von [6], Hellingman P. [6], Hellsten T.[1-10], Hemming O.N.[15], Hemsworth R.[2], Hender T.[15], Henderson M.[12], Hennequin P.[2], Henshaw A.[15], Herrmann A. [8], Hidalgo C. [3], Hill J.[15], Hillis D.[19], Hitchin M.[15], Hoang T.[2], Hobirk J. [8], Hoekzema F. [7], Hoekzema J.A. [7], Hofmann F.[12], Hogan C.[19], Hogben C., H.A.[15], Hogeweij D. [6], Horton A.[15], Horton L.D. [8], Hosea J.[18], Hoskins A.J.[15],

Hough M.R.[15], Houlberg W.[19], How J.[2], Howell D.[15], Hron M.[24], Huber A. [7], Hudson Z.[15], Hume H.[15], Hurd F.[16], Hutchinson I.[21], Hutter T.[2], Huygen S.[23], Huysmans G.[2], Imbeaux F.[2], Ingesson C. [6], Innocente P. [5], Jachmich S.[23], Jackson G.[20],Jacquinot J.[2], Jarmen A.[10], Jarvis N.[15], Jaspers R. [6], Jaun A.[10], Jenkins I.[15], Jensen H.S.[14], Joffrin E.[2], Johnson M.[15], Johnson R.[15],Jones E.M.[15], Jones G.[15], Jones H.D.[15], Jones T.[15], Jonsson T.[10], Jupen C.[10],Kallenbach A. [8],Kallne J.[10], Karttunen S.[13], Kasparek W.[14], Kaye A.[15], Kelliher D. [4], Kemp N.[15], King R.F.[15], Kiptily V.[15], Kirov K. [8], Kirschner A. [7], Kiviniemi T.[13], Knight P.[15], Knipe S.[15], Koch R.[23], Kooijman W.[6], Korotkov A.[15], Koslowski H-R [7], Kramer G.[18],Kraus W. [8], Kruijt O.G.[6], Kurki Suonio T.[13], Lackner K.[16], Laesser R. [7], LaHaye R.J.[20], Lam N.[15], Lamalle Ph.[1-23], Land G. [6], Lang P. [8], Last J.[15], Laux M. [8], Laviron C.[2], Lawson K.[15], Laxaback M.[10], Lazzaro E. [5], Lehnen M. [7],Leigheb M. [5], Lescure C.[15], Leuterer F. [8], Likin K.[3], Likonen J.[13], Lingier K. [6], Linke J. [7], Lister J.[12], Litaudon X.[2], Lloyd B.[15], Lloyd G.[15], Loarer T.[2], Loarte A.[16], Lomas P.[15], Lönnroth J.[13], Lorenz Axel[1], Lotte P.[2],Louche F.[23], Loughlin M.[15], Loving A.[15], Lucock R.M.A.[15], Lyssoivan A.[23], Maagdenberg J.[6], Maas A.[2], MacGregor J.[15], Macheta P.[15], Maddaluno G. [5], Maddison G.[15], Maget P.[2], Magne R.[2], Mailloux J.[15], Maisonnier D.[16], Mank G. [7], Manso M.Emilia [9], Mantica P. [5], Mantsinen M.[13], Maraschek M. [8], Marcuzzi D. [5], Marinucci M. [5], Marmillod Ph.[12], Marmillod Philippe[12], Martin D.[15], Martin Y.[12], Mattei M. [5],Matthews G.[15], Mayer M. [8], Mayoral M-L.[15], Mazon D.[2], Mazzone G. [5], Mazzucato E.[18], McCarron E. [15], McClements K.[15], McCormick K. [8], McCullen P.A.[15], McDonald D.[15], Mead M.[15], Medina F. [3], Meigh S.[15], Meigs A.[15], Melissen W. [6], Meneses L. [9], Meo F. [8], Mertens Ph. [7], Mertens V. [8], Messiaen A.[23], Middelton R.[15], Milani F.[15], Mills S.[15], Milnes J.[15], Minh Quang Tran[12], Mlynar J.[12], Monakhov I[15], Monier-Garbet P.[2], Monk R. [8], Moreau D.[2],Moreau Ph.[2], Morgan P.[15], Morris J.[15], Morris W.[15], Mort J.L.[15], Mück A. [8], Mueller G.[14], Murari A. [5], Murdock D.[16], Nabais F. [9], Nave M.F.F Nave [9], Nazikian R.[18], Negus Clive[15], Neil G.[15], Neilson J.D[15], Neu R. [8], Newbert G.J.[15], Nguyen F.[2], Nichols K.[15], Nicholson C.[15], Nicolai A. [7], Nicolas L.[2], Nielsen Per [5], Nightingale M.[15], Nordman H.[10], Noterdaeme J-M. [8], Nowak S. [5], Ogawa M. T.[22], O'Mullane[15], Ongena J.[23], Orchard J.[15],Orsitto F.[1-5], Pale P.[1-13], Palmer J.[16], Pamela J.[1-2], Panaccione L. [5], Parail V.[15], Parsons B.[15], Pasqualotto R. [5], Patel B.[15], Pavlenko I[23], Peacock A.T.[16], Pearce R.[15], Pecquet A-L.[2], Pedrosa Luna A. [3], Peeters A. [8], Penzhorn R.D.[14],Peres Alonso M. [9], Pereverzev G. [8], Perevezentsev A.[15],Perez von Thun C [7], Pericoli V. [5], Peruzzo S. [5], Petravich G.[26], Petrizilka V.[24], Phillips V. [7], Pick M.[16], Pinches S. [8], Pinna T. [5], Piosczyk B.[14], Piosczyk B.[14] , Pitcher S.[21], Pitts R.[12], Plysnin V. [9], Pochelon A.[12], Podda S. [5], Polinari P. [5], Pomaro N. [5], Pool P.J.[15], Popovichev S.[15], Portafaix C.[2],Pospieszczyk A. [7], Preece G.[15], Prentice R.[15], Prins R. [6], Proschek M.[11], Pugno R. [8], Puiatti M-E. [5], Purahoo K.[15], Rachlew E.[10], Rainford M.[15], Rapp J. [7], Reiser D. [7], Reitano G. [5],Reiter D. [7], Ribeiro T-M. [9], Riccardo V.[15], Righi E.[16], Rimini F.G.[2], Riva M. [5], Robinson S.A.[15], Robson D.W.[15], Roccella M. [5], Rodriguez L. [3], Rogero G[2], Rogister A. [7], Rolfe A.[15], Ronden D.[6], Roquemore L.[18], Rosanvallon S.[2], Ross D[15], Rubel M.[10], Ryter F. [8], Saarelma S.[13], Sabathier F.[2], Sabot R.[2], Saibene G.[16], Sakurai S.[22], Salavy J-F.[2], Sall I.[15], Sanchez J. [3], Sanders S.[15], Sands D.[15], Sarazin Y.[2], Sartori R. [16], Sartori F. [15], Sattin F. [5], Sauter O.[12], Sborchia C.[16], Scarabosio A.[12],Schlosser J.[2], Schmidt G.[18], Schmidt W. [5], Schüller C. [6], Schweer B. [7],Schweinzer J.[1-8], Segui J.L.[2], Semeraro L. [5], Sergienko G. [7], Serra F. [9], Sharapov S.[15], Shaw S.R.[15], Shimizu K.[22], Siegrist M.[1-12], Silva C-A. [9], Simpson D.[15], Sipila S.[13], Sips A.C. [8], Sjostrand H.[10], Smith P.G.[15], Snipes J.[21],Solano E.R.[1-3], Sonato P. [5], Sousa J. [9], Sozzi C. [5], Spelzini A.M.[15], Spence J.[15], Speth E. [8], Staebler A. [8], Stafford-Allen R.[15], Stagg R.[15], Stakenborg J.[6], Stamp M.[15], Starkey D.[15], Stephen A.[15], Sterk A. [6], Sterk A.B. [6], Stevens A.[15], Stober J. [8], Stokes R.[15], Stork D.[15], Storrs J[15], Strachan J.[18], Stratton K.[18], Stubberfield P.[15], Summers D.[15], Surrey E[15], Sutton D.[15], Suttrop W. [8], Symonds I.[15],Tabares F. [3],Tait J.[15], Takeji S.[22], Tala T.[13], Talarico C. [5],Talbot A.R.[15], Taliercio C. [5], Tam U. [7], Tame C.[15], Tardini G. [8], Tardocchi M.[10], Tartoni N. [5], Tavernier J.[2], Telesca G. [5], Terrington A.O.[15], Testa D.[21-12], Testoni P. [5], Thomas P.[1-2],

Thomsen H. [8], Thomsen K.[16], Thumm M.[14], Tichler J. [6], Tigwell P.[15], Tiscornia T.[15], Titus P.[21], Todd J.M.[15], Tokar M.Z. [7],Tran M.Q.[12], Travere J-M.[2], Tresset G.[2], Tribaldos V. [3], Tsitrone E.[2], Tuccillo A.A. [5], Tudisco O. [5], Turner M [4], Udintsev V. [6], Unterberg B. [7],Valetta M.P.[2], Valisa M. [5], Valovic M.[15], van Amerongen F.[6],vandePollMarc [6], Van der Grift T. [6],Van Eester D.[23],Van Gorkorm J. [6], Varela P. [9],VenderDavid[4],Veres G.[25], Verhoeven A. [6], Villard Laurent[12], Villedieu E.[2], Villone F. [5],VonHellerman M. [6], Vulliez K.[2], Wagner Dietmar [8], Walden A.[15], Walker M.[15], WaltonB.[15],Watkins M.L.[1-15], Watson M.J.[15], Way M.[15], Weiland J.[10],Weisen H.[12], WernerAndreas[8], Wesner F. [8], Westerhof E. [6], Weyssow B.[23], Wheatley M.R.[15], Whitehurst A.[15], Wicks S.J.[15], Widdershoven L. [6], Wienhold P. [7], Wilson A.[15], Wilson C.[15], Wilson D.[15], Wilson D.J.[15], Wilson D.W.[15], Wilson R.[18], Wischmeier M.[12],Wolf R. [8], Wouters P.[23], Yorkshades J.S.[15], Young C.[15], Young D.[15], Young I.D.[15], Young K.[18], Zabeo L. [5], Zacek F.[24], Zanca P. [5], Zastrow K-D.[15], Zeidner Wolfgang [8], Zerbini M. [5], Zohm H. [8], Zoletnik S.[25], Zoletnik S.[25], Zonca F. [5], Zwingman W.[2]

[1] EFDA Close Support Unit, Culham, *UK*.
[2] Association Euratom-CEA, Cadarache, *France*.
[3] Association EURATOM-CIEMAT para Fusion, Madrid, *Spain*.
[4] Dublin City University (DCU), *Ireland*.
[5] Associazione Euratom ENEA sulla Fusione, Frascati, Roma, *Italy*.
[6] FOM-Rijnhuizen, Association Euratom-FOM, TEC, Nieuwegein, *The Netherlands*.
[7] Institut fur Plasmaphysik, Forschungszentrum J®ulich, Trilateral Euregio Cluster, D-52425 Julich, *Germany*.
[8] Max-Planck-Institut für Plasmaphysik, EURATOM-Assoziation, D-85748 Garching, *Germany*.
[9] Euratom/IST, Instituto Superior Técnico, Lisbon, *Portugal*.
[10] Euratom-VR Association, Swedish Research Council, Stockholm, *Sweden*.
[11] Österreichische Akademie der Wissenschaften (ÖAW), *Austria*.
[12] Centre de Recherches en Physique des Plasmas, Association EURATOM-Confédération Suisse, EPFL, 1015 Lausanne, *Switzerland.*
[13] Helsinki U. of Technology, Tekes-Euratom Assoc., PO Box 2200, FIN-02015 HUT, *Finland*.
[14] Forschungszentrum Karlsruhe (FZK), *Germany*.
[15] Euratom/UKAEA Fusion Association, Culham, Abingdon, *UK*.
[16] EFDA Close Support Unit, Garching, *Germany*.
[17] ITER Joint Central Team, Garching, *Germany*.
[18] Princeton Plasma Physics Laboratory, New-Jersey, *USA*.
[19] Oak Ridge National Laboratory, Tennessee, *USA*.
[20] General Atomics, San-Diego, California, *USA*.
[21] Massachusetts Institute of Technology, Cambridge, Massachusetts, *USA*.
[22] JAERI, Naka, *Japan*.
[23] Association Euratom-Belgian State, LPP-ERM/KMS, *Belgium*.
[24] Institute of Plasma Physics (IPP), Academy of Sciences, *Czech Republic*.
[25] Hungarian Academy of Sciences (HAS), *Hungary*.
[26] Ministry of Education and Research (MEC), *Romania*.
[27] Université de Nice-Sophia-Antipolis, Nice, *France*.
[28] Colorado School of Mines (CSM), *USA*.